JOURNAL OF VIROLOGY, Jan. 1996, p. 47–54 Vol. 70, No. 1
0022-538X/96/$04.00+0

Phenotypic Characterization of Mutants in Vaccinia Virus Gene G2R, a Putative Transcription Elongation Factor

E. PENELOPE BLACK AND RICHARD C. CONDIT*

Department of Molecular Genetics and Microbiology and Center for Mammalian Genetics, University of Florida, Gainesville, Florida 32610-0266

Received 10 August 1995/Accepted 26 September 1995

The phenotypic defects of two mutants of vaccinia virus, the lesions of which map to gene G2R, were characterized in vivo, and the results suggest a role for the G2R protein in viral transcription elongation. Both a temperature-sensitive mutant, C*ts*56, and an isatin-β-thiosemicarbazone-dependent deletion mutant, G2A, in gene G2R have a characteristic and unique defect in late viral gene expression. The G2R mutants synthesize early viral RNA, early viral proteins, and viral DNA normally under nonpermissive conditions. In G2R mutants, late viral protein synthesis begins at the normal time, low-molecular-weight viral proteins are synthesized in normal quantities, but synthesis of high-molecular-weight viral proteins is reduced in amount. Intermediate and late promoter utilization is normal in G2R mutants, but intermediate and late RNAs are reduced in size. The reduction in length of the intermediate and late mRNAs represents a truncation of mRNA 3′ ends. Thus, intermediate and late RNAs are too short to encode large proteins but long enough to encode small proteins, therefore accounting for the protein synthesis phenotype. These results suggest that the G2R protein acts to regulate the elongation potential of the viral RNA polymerase late during a vaccinia virus infection.

Vaccinia virus, the prototypic member of the orthopoxvirus family, unlike other DNA viruses, carries out its nucleic acid synthesis in the cytoplasm of infected cells (19). The virus encodes the vast majority of enzymes necessary for viral DNA and mRNA synthesis and modification; thus, the contribution of the host cell nucleus to nucleic acid metabolism is minimal (21, 24). Many of the enzymes involved in vaccinia virus nucleic acid metabolism bear structural and functional similarities to host cell enzymes; thus, vaccinia virus provides a simple model system for genetic and biochemical analysis of eucaryotic nucleic acid metabolism.

Vaccinia virus gene expression is controlled primarily at the level of transcription. Vaccinia virus genes are transcribed in a cascade composed of three distinct gene classes: early, intermediate, and late (2, 13). All three gene classes are transcribed by the same multisubunit core viral RNA polymerase. Individual gene classes are distinguished by a discrete set of biochemically and genetically well defined promoter elements and *trans*-acting transcription initiation factors (20). The structures of intermediate and late vaccinia virus mRNAs differs significantly from the structure of early viral mRNAs primarily as a result of differences in the formation of mRNA 3′ ends (15). Early gene transcription is actively terminated at a conserved sequence element in the mRNA in a process catalyzed by a virus-coded *trans*-acting factor (26, 28). Early viral mRNAs are therefore discrete in size, with homogeneous 5′ and 3′ ends. In contrast, at intermediate and late times during infection, early termination signals are ignored, and intermediate and late transcripts do not appear to be terminated at unique sites on the genome (15). Intermediate and late transcripts are therefore heterogeneous in length, with discrete 5′ ends and heterogeneous 3′ ends.

We have taken a genetic approach to studying regulation of gene expression in vaccinia virus. Pursuant to this goal, we have isolated and mapped a number of conditional lethal mutants of vaccinia virus and conducted phenotypic analysis of several of these mutants that display defects in gene expression (7). Preliminary characterization of mutants in gene G2R showed a defect in late viral protein synthesis under nonpermissive conditions (6, 16). Characterization of the G2R gene predicts that it encodes a 26-kDa protein that is expressed early during infection. The predicted amino acid sequence of G2R contains no recognizable functional motifs and shows no significant homologies to other proteins currently in published protein databases.

Studies on the mechanism of action of the antipoxvirus drug isatin-β-thiosemicarbazone (IBT) imply that gene G2R affects viral transcription. In wild-type (wt)-infected cells, IBT induces promiscuous transcription, that is, transcriptional activation late during infection of regions of the genome which are normally transcriptionally silent (3). Inactivation of gene G2R results in a virus which is dependent on IBT for growth, demonstrating that inactivation of gene G2R compensates for or counteracts promiscuous transcription (17). To further test the hypothesis that G2R plays a role in viral transcription, we have conducted a detailed phenotypic analysis of mutations in vaccinia virus gene G2R. The results reported here suggest that the G2R protein influences viral transcription elongation.

MATERIALS AND METHODS

Cells and viruses. BSC40 cells, vaccinia viruses C*ts*56 and G2A, and the conditions for virus growth, infection, and plaque titration have been described previously (5, 6, 17). IBT was prepared as described previously (22) and used at a final concentration of 45 μM.

Riboprobes. Reactions for synthesis of antisense riboprobes were done essentially as described in the Promega "Protocols and Applications Guide," using either linearized plasmid DNA or PCR products as templates for T7 or SP6 RNA polymerase (Table 1). Riboprobes had a specific activity of 2×10^8

* Corresponding author. Mailing address: Department of Molecular Genetics and Microbiology and Center for Mammalian Genetics, University of Florida, Box 100266, Gainesville, FL 32610-0266. Phone: (904) 392-3128. Fax: (904) 392-3133. Electronic mail address: condit@icbr.ifas.ufl.edu.

cpm/μg. The probes were used for both Northern (RNA) blot analysis and RNase protection studies. Plasmid and PCR templates are described separately below and in Table 1.

Plasmids 1 to 3 (Table 1) were kindly provided by Bernard Moss (1). Plasmids 4 to 7 were constructed by PCR amplification of the indicated region of either gene A10L or gene F17R, using primers that contain sequences complementary to vaccinia virus genomic DNA and additional restriction sites for cloning. Amplified DNA fragments were cloned into the plasmid vector pGEM3Zf−, using standard techniques (25).

Templates 8 to 11 (Table 1) are double-stranded DNA molecules produced by PCR, using primers complementary to indicated vaccinia virus sequences. In each case, the downstream primer contained the consensus T7 RNA polymerase promoter sequence, 5′ tgTAATACGACTCACTATA 3′ (uppercase letters represent the T7 RNA polymerase promoter, and the lowercase letters represent extra nucleotides deemed necessary for efficient T7 RNA polymerase binding) (18). PCR products were purified on 10% polyacrylamide–50% urea gels.

Protein pulse-labeling. Pulse-labeling of proteins in virus-infected cells was done as described previously (5). Briefly, confluent monolayers of BSC40 cells in 35-mm-diameter dishes were infected with vaccinia virus at a multiplicity of infection (MOI) of 15 or mock infected. At various times after infection, cells were metabolically labeled with 10 μCi of Tran[^{35}S]-label (ICN Biochemical, Irvine, Calif.) in 0.5 ml of phosphate-buffered saline (PBS). Cells were lysed on the dishes by addition of sodium dodecyl sulfate (SDS)-polyacrylamide gel electrophoresis (PAGE) sample buffer, and solubilized proteins were analyzed by SDS-PAGE, using 10% separating gels (14). The gels were Coomassie blue stained, dried, and autoradiographed. For Fig. 1C, proteins were quantified with a Molecular Dynamics, Inc., model 400S PhosphorImager.

DNA accumulation. Accumulation of viral DNA in vaccinia virus-infected cells was measured essentially as described by Ensinger (9). Briefly, confluent monolayers of BSC40 cells in 35-mm-diameter dishes were infected at an MOI of 15 with wt or mutant virus. At various times after infection, the cells were washed with PBS, scraped from the dishes, and concentrated by centrifugation. The cells were resuspended in 0.3 ml of loading buffer (10× SSC [1× SSC is 0.15 M NaCl plus 0.015 M sodium citrate] containing 1 M ammonium acetate). The samples were frozen and thawed three times and diluted with 4 volumes of loading buffer. One microliter of each sample was then denatured by dilution into 100 μl of a solution containing 0.25 N NaOH and 0.5 M NaCl and incubation at room temperature for 10 min. Ten microliters of each denatured sample was diluted into 990 μl of a solution containing 0.1× SSC and 0.125 N NaOH. One hundred microliters of each sample was then loaded onto a GeneScreen (New England Nuclear) membrane, using a Schleicher & Schuell slot blot apparatus, and filters were washed and UV cross-linked according to the GeneScreen instructions. The membrane was hybridized with an excess of *Hin*dIII-digested genomic vaccinia virus DNA labeled with [α-^{32}P]dCTP by random priming (10). Hybridizations were done in 50% formamide hybridization buffer as described in the GeneScreen manual.

Northern blot analysis. RNA was purified from infected cells essentially as described previously (3). Briefly, confluent monolayers of BSC40 cells in 100-mm-diameter dishes were infected at an MOI of 15 with mutant or wt virus. At various times after infection, cells were harvested in 1 ml of GTC buffer (4 M guanidine thiocyanate, 0.1 M Tris-HCl [pH 7.5], 0.5% Sarkosyl, 0.1 M mercaptoethanol). RNA samples were pelleted through a CsCl cushion (5.7 M CsCl, 0.01 M EDTA [pH 7.5]) for 24 h in a Beckman SW55 rotor at 35,000 rpm. The RNA pellet was dissolved, precipitated with ethanol, resuspended in water, and quantitated by measuring the A_{260}.

Purified RNA was denatured in formamide and electrophoresed through 1.2% formaldehyde-agarose gels as described previously (25). RNAs were transferred, prehybridized, and hybridized, and radioactivity associated with each lane was quantitated by PhosphorImager analysis as previously described (3).

RNase protection analysis. Ten micrograms of total RNA isolated from infected cells was added to 5 ng of [^{32}P]CTP-labeled riboprobe, and the mixture was precipitated with 0.3 M sodium acetate and 2.5 volumes of ethanol at −20°C. The precipitated RNA was redissolved in 30 μl of hybridization buffer [40 mM piperazine-*N*,*N*′-bis(2-ethanesulfonic acid) (PIPES; pH 6.4), 1 mM EDTA, 400 mM NaCl, 80% formamide], heated for 5 min at 85°C, and then incubated at 42°C overnight. Following hybridization, 300 μl of digestion buffer (10 mM Tris-HCl [pH 7.5], 5 mM EDTA, 300 mM NaCl, 4 μg of RNase A per ml, 10 U of RNase T_1 per ml) was added, and samples were incubated at 37°C for 1 h. After RNase digestion, 20 μl of a solution containing 10% SDS and 100 μg of proteinase K was added, and samples were incubated at 37°C for an additional 15 min. The entire reaction mixture was then extracted with phenol-chloroform, and the aqueous layer was removed and precipitated with 1 μl of glycogen (20 mg/ml) and 1 ml of 100% ethanol at −20°C. The precipitated RNA pellet was resuspended in 10 μl of stop solution (95% formamide, 20 mM EDTA, 0.05% bromophenol blue, 0.05% xylene cyanol), heated for 5 min at 70°C, and electrophoresed through a 6% acrylamide–8 M urea gel (Sequagel; National Diagnostics). The gel was dried and autoradiographed.

RESULTS

G2R mutant viruses. The sequence of the G2R gene predicts a protein 221 amino acids in length. Conditional lethal mutants of vaccinia virus with lesions mapping to the G2R gene have been isolated previously (17). One mutant, designated C*ts*56, was isolated during a large-scale screen for vaccinia virus mutants which were temperature sensitive (*ts*) for plaque formation (6). C*ts*56 contains a single nucleotide change of a G to an A at nucleotide (nt) 451 (codon 151), resulting in an amino acid change from glycine to arginine in the G2R gene. C*ts*56 has a complex growth phenotype. One-step growth experiments have confirmed that in the absence of IBT, this virus is *ts* for growth (11). In the presence of IBT, C*ts*56 grows at both 31 and 40°C, the permissive and nonpermissive temperatures for growth in the absence of the drug. Thus, C*ts*56 is IBT resistant at 31°C and IBT dependent at 40°C (17). The second mutant, an IBT-dependent deletion mutant designated G2A, contains a 10-bp deletion from nt 268 to 277 (codons 90 to 93) that results in a frameshift beginning at codon 90 and a translation stop at codon 93. This virus is unable to form plaques at 37°C in the absence of IBT (17).

Protein synthesis in mutant-infected cells. Protein pulse-labeling experiments were done to characterize the pattern of viral gene expression in G2R mutant-infected cells. Monolayers of BSC40 cells were pulse-labeled with [^{35}S]methionine at various times following infection with either wt or G2R mutant

TABLE 1. Riboprobes

Construct no.	Riboprobe	Gene (class)[a]	Template	Coding size (bp)	Position[b]				Probe 3′ vector sequence (nt)	Probe 5′ vector sequence (nt)	Probe length (nt)	Protected length (nt)
					ATG	Translation stop	Probe 3′	Probe 5′				
1	pGEM-VGF	C11R (E)	Clone	425	+59	+480	−322	+316	ND[c]	ND	678	316
2	pGEM-30K	G8R (I)	Clone	779	+5	+784	−200	+300	ND	ND	530	300
3	pGEM-11K	F17R (L)	Clone	330	+4	+307	−544	+126	ND	ND	682	126
4	pPB4a5′	A10L (L)	Clone	2,672	+4	+3144	+4	+173	5	43	225	177
5	pPB4a3′	A10L (L)	Clone	2,672	+4	+3144	+2504	+2657	0	11	164	153
6	pPB11K5′	F17R (L)	Clone	330	+4	+307	−4	+143	8	26	173	139
7	pPB11K3′	F17R (L)	Clone	330	+4	+307	+165	+310	8	26	179	145
8	4a-5′	A10L (L)	PCR	2,672	+4	+3144	+4	+89	6	6	97	85
9	4a-nt 1000	A10L (L)	PCR	2,672	+4	+3144	+993	+1115	6	6	134	122
10	4a-nt 2000	A10L (L)	PCR	2,672	+4	+3144	+2012	+2172	6	6	172	160
11	4a-3′	A10L (L)	PCR	2,672	+4	+3144	+2414	+2624	6	6	222	210

[a] E, early; I, intermediate; L, late.
[b] Relative to mRNA 5′ end at +1.
[c] ND, not determined.

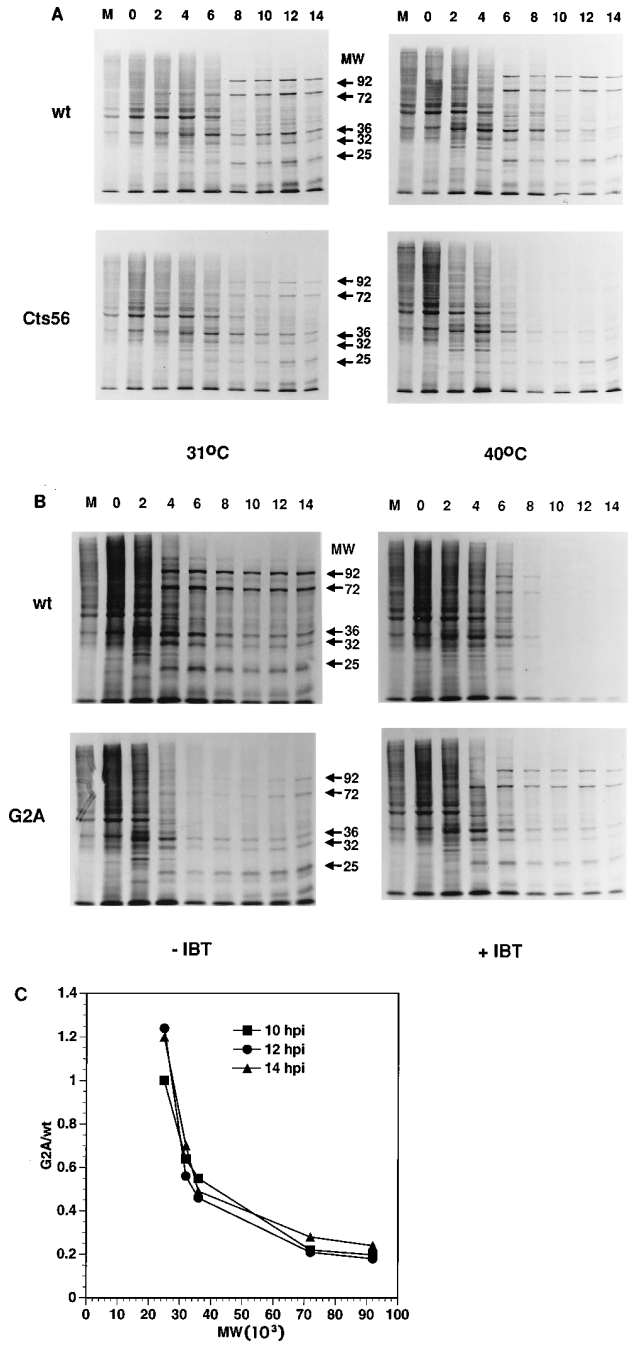

FIG. 1. Protein synthesis in wt- and G2R mutant-infected cells. BSC40 cells were infected with wt or G2R mutant virus at an MOI of 15 and then pulse-labeled for 15 min with Tran[^{35}S]-Label at the times postinfection (hours) indicated above the lanes. Lane M, mock infection. Infected cells were harvested, electrophoresed on SDS–10% polyacrylamide gels, and autoradiographed. (A) Top panels, wt; bottom panels, C*ts*56; left panels, 31°C; right panels, 40°C. (B) Top panels, wt; bottom panels, G2A; left panels, incubation at 37°C in the absence of IBT; right panels, incubation at 37°C in the presence of 45 μM IBT. Molecular weights (MW) are given in thousands. (C) Proteins designated by the arrows in panel B were quantified by PhosphorImager analysis. Graphical representation of the 10-, 12-, and 14-h postinfection (hpi) time points are shown as a ratio of G2R mutant to wt protein.

virus, and the labeled proteins were analyzed by SDS-PAGE and autoradiography (Fig. 1). The wt infections shown in Fig. 1A and B illustrate the normal pattern of viral protein synthesis at 31 and 40°C (permissive and nonpermissive conditions for *ts* mutants; Fig. 1A) and at 37°C in the absence of IBT (nonpermissive conditions for the G2R deletion mutant G2A; Fig. 1B). In wt-infected cells, host protein synthesis is shut off within 4 to 6 h postinfection. Early viral protein synthesis, best represented in these experiments by a protein of approximately 30 kDa, begins by 2 h postinfection, peaks between 2 and 4 h postinfection, and is shut off by 6 to 8 h postinfection. Late viral protein synthesis, represented best by five proteins ranging in molecular mass from 25 to 92 kDa (Fig. 1A and B), begins between 4 and 6 h postinfection and continues throughout the experiment. During infection with C*ts*56 under permissive conditions (31°C; Fig. 1A), the schedule of host shutoff and viral protein synthesis is virtually identical to that for the wt virus infection; however, synthesis of late proteins is slightly reduced in quantity. During infection with C*ts*56 under nonpermissive conditions (40°C; Fig. 1A), the schedule of host shutoff and viral protein synthesis is also virtually identical to that for the wt virus infection; however, synthesis of large late proteins is drastically reduced, while small late proteins seem to be synthesized in normal amounts. Infection with the G2R deletion mutant G2A under nonpermissive conditions (Fig. 1B, −IBT) results in a pattern of viral protein synthesis which is strikingly similar to that for the C*ts*56 infection done under nonpermissive conditions. As expected, addition of IBT to the G2A infection restores the expression of large late viral proteins to near wt levels (Fig. 1B). As described previously, infection with wt virus in the presence of IBT induces promiscuous transcription, which in turn results in overproduction of double-stranded RNA, stimulation of the 2-5A pathway, and cessation of protein synthesis late during infection (3). In summary, these results indicate that during infection with G2R mutants, host shutoff and early viral protein synthesis are normal, late viral protein synthesis begins at the normal time, low-molecular-weight late viral proteins are synthesized in normal quantities, but synthesis of high-molecular-weight late viral proteins are reduced in amount.

To confirm that synthesis of high-molecular-weight viral proteins was specifically defective in G2R mutant-infected cells, synthesis of each of the five late proteins designated in Fig. 1B was quantified with a PhosphorImager. Quantities of each of the five proteins synthesized in either G2A or wt infections were determined by using the 10-, 12-, and 14-h pulse-labeling time points shown in Fig. 1B. Figure 1C shows that for each time point, equal quantities of the 25-kDa protein were synthesized in wt- and G2R mutant-infected cells and that the ratio of G2A to wt protein synthesis decreased as the apparent molecular weight of the proteins increased.

Viral DNA accumulation in mutant-infected cells. Because intermediate and late viral gene expression is coupled to viral DNA replication, any defect in late viral protein synthesis could theoretically result indirectly from a defect in viral DNA replication. Viral DNA accumulation in infected cells was therefore measured to determine if the G2R mutants were defective in viral DNA synthesis. To assay viral DNA accumulation, BSC40 cells were infected with either wt or G2R mutant virus, and at various times following infection, total cell lysates were prepared. The lysates were denatured in alkali, blotted to a GeneScreen membrane by using a slot blot apparatus, and hybridized to an excess of random-primed vaccinia virus genomic DNA. The hybridization was quantified with a PhosphorImager. The results (Fig. 2) show that the kinetics of DNA accumulation in G2R mutant infections done under nonpermissive conditions are not significantly different from the kinetics of DNA accumulation observed during G2R infections done under permissive conditions or during a wt infection. Therefore, it seems unlikely that a defect in DNA replication

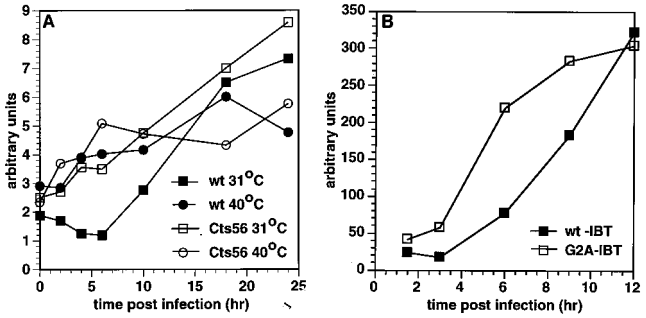

FIG. 2. DNA accumulation in wt- and G2R-infected cells. BSC40 cells were infected with wt or G2R mutant virus at an MOI of 15; crude cell extracts were made, denatured in alkali, and slot blotted onto GeneScreen membranes. The membranes were probed with [^{32}P]dCTP-labeled vaccinia virus DNA and autoradiographed. Bound probe was quantified by PhosphorImager analysis. −IBT, absence of IBT.

is responsible for the protein synthesis phenotype observed in the G2R mutant-infected cells.

Steady-state mRNA levels in mutant-infected cells. The protein synthesis profile in G2R mutant-infected cells could be explained by a deficiency in viral mRNA metabolism. Northern blot analysis was therefore used to measure the quantity, size, and kinetics of synthesis of early, intermediate, and late viral mRNAs in G2R mutant-infected cells. Monolayers of BSC40 cells were infected with either wt or G2A mutant virus, and total RNA was purified from the infected cells at various times postinfection. Equal amounts of total RNA were fractionated on formaldehyde-agarose gels and transferred to GeneScreen, and the RNAs of interest were detected by using riboprobes (Table 1, probes 1 to 3) specific for the 5′ ends of an early (C11R), an intermediate (G8R), or a late (F17R) gene (Fig. 3). The wt time course illustrates both the expected size distribution and kinetics of synthesis of viral mRNA for each probe used. Specifically, the early C11R mRNA (Fig. 3A) is synthesized as a discrete band which appears by 1.5 h postinfection, peaks at 6 h postinfection, and disappears by 12 h postinfection. The intermediate G8R mRNA (Fig. 3B) is synthesized as a smear which appears by 6 h postinfection, peaks at 9 h postinfection, and decreases at 12 h postinfection. The late F17R mRNA (Fig. 3C) is synthesized as a smear which appears by 6 h postinfection and persists at high levels throughout the experiment. In the G2A mutant-infected cells, the synthesis of the early C11R mRNA is identical to that in wt infections. By contrast, in G2A mutant-infected cells, the intermediate G8R and late F17R mRNAs are synthesized in similar amounts and at similar times compared with the wt infection, but the mRNAs are reduced in size. The absolute sizes of the intermediate and late RNAs made in G2A-infected cells are similar, approximately 300 to 1,500 nt. Significantly, this size is large enough to encode proteins in the size range of 10 to 50 kDa but too small to encode proteins with sizes greater than 50 kDa.

To determine whether promoter utilization is normal in G2R mutant infections, mRNA 5′-end analysis was done by using RNase protection performed with the same early, intermediate, and late gene riboprobes used in the Northern blot analysis described above (Table 1, probes 1 to 3). Total infected-cell RNA was hybridized to an excess of uniformly labeled antisense riboprobe, and the hybrids were digested with RNase in high salt, denatured, and analyzed by electrophoresis on polyacrylamide-urea gels and autoradiography (Fig. 4). The riboprobes used contain antisense RNA sequence from both upstream and downstream of the previously determined

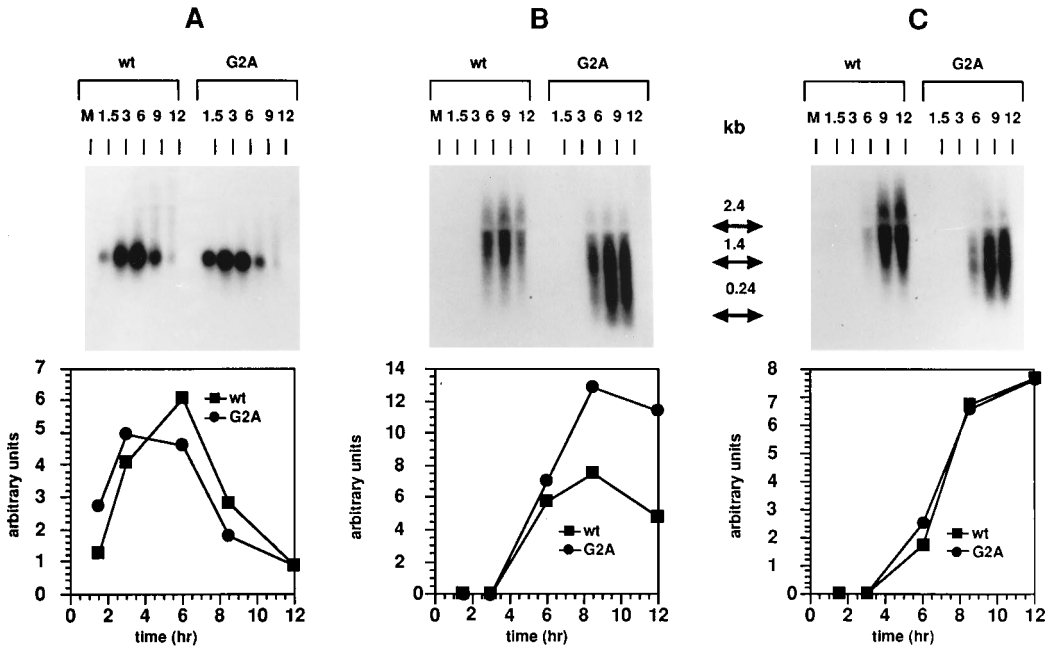

FIG. 3. Northern blot analysis of RNA synthesized in wt- and G2A mutant-infected cells. BSC40 cells were infected with wt or G2A mutant virus at an MOI of 15, and infected cells were harvested at the times postinfection (hours) indicated above the lanes. Total RNA was purified on CsCl gradients, and equal amounts of RNA were fractionated on formaldehyde-agarose gels, transferred to GeneScreen membranes, and probed with uniformly labeled antisense RNA riboprobes specific for an early, C11R (Table 1, probe 1) (A), an intermediate, G8R (Table 1, probe 2) (B), and a late, F17R (Table 1, probe 3) (C), viral mRNA. Arrows between panels B and C indicate the positions of RNA size markers. Lanes M contain uninfected cell RNA. Below each autoradiograph is the PhosphorImager quantification of hybridized mRNA at each time point.

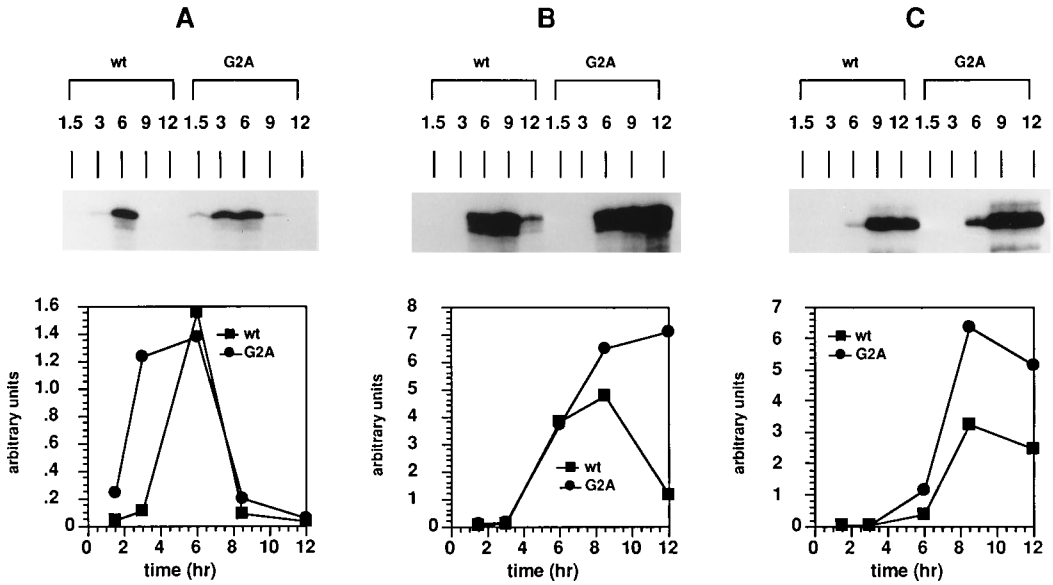

FIG. 4. Analysis of viral mRNA 5′ ends in wt- and G2A mutant-infected cells by RNase protection. Total RNA was isolated from infected BSC40 cells at the times indicated and was hybridized to uniformly labeled antisense RNA specific for the 5′ end of the early, C11R (Table 1, probe 1) (A), the intermediate, G8R (Table 1, probe 2) (B), or the late, F17R (Table 1, probe 3) (C), gene. After RNase digestion, the protected probe fragments were analyzed by denaturing PAGE and autoradiography. PhosphorImager quantification of the expected protected fragments for each probe in both wt and mutant infections is shown below each autoradiograph.

mRNA 5′ ends (Table 1). The sizes of the protected fragments shown in Fig. 4 correspond precisely to the mRNA 5′ ends previously determined for each gene tested (1). In wt infections (Fig. 4), the kinetics of appearance of 5′-end protected fragments for each gene were similar to the kinetics of mRNA synthesis detected by Northern blot analysis (Fig. 3). In G2A infections (Fig. 4), protected fragments which are the same size as those detected in the wt infection were detected, and the fragments appear with similar kinetics and in similar amounts compared with the wt infection. We interpret these data to mean that for the C11R, G8R, and F17R genes, promoter utilization in the G2R-mutant infected cells is normal compared with a wt infection. Thus, the defects in late protein synthesis and intermediate and late mRNA synthesis observed in G2R mutant infections cannot be explained by a defect in initiation of early, intermediate, or late transcription.

Since in G2R mutant-infected cells, intermediate and late promoter utilization is normal but mRNAs are abnormally short, we hypothesize that the reduction in mRNA size represents a truncation of mRNA 3′ ends. Furthermore, since the defect appears to affect synthesis of large but not small proteins, we hypothesize that a truncation of mRNA 3′ ends would affect the 3′ coding sequences of large but not small genes. We tested this hypothesis first by performing Northern blot analysis using probes specific for the 5′ and 3′ ends of a small (F17R) and a large (A10L) late gene. The sequences chosen for the riboprobes represent in each case the 5′ and 3′ ends of the protein coding sequence and do not contain 5′ or 3′ untranslated sequences (Table 1, probes 4 to 7). For the F17R gene (Fig. 5A and B), the Northern blots prepared by using either the 5′ (Fig. 5A) or the 3′ (Fig. 5B) riboprobe are similar to the Northern blots for the F17R gene presented in Fig. 3C. Specifically, with either probe, the RNAs detected in G2A-infected cells appear with similar kinetics and in similar amounts compared with wt infections but are reduced in size. Most importantly, the result obtained with the 3′ probe is virtually identical to the result obtained with the 5′ probe. Northern blot analysis of RNA from wt- and G2A-infected cells by using the gene A10L 5′ probe (Fig. 5C) reveals a pattern of RNA metabolism which is similar to the pattern observed for the G8R gene (Fig. 3B) and the 5′ and 3′ ends of the F17R gene (Fig. 3C and 5A and B). Specifically, RNA detected by the A10L 5′ probe appears with similar kinetics and in similar amounts in wt- and G2A-infected cells, but in G2A infections, the RNA is smaller than in the wt infection. The results with the A10L 3′ probe (Fig. 5D) are distinctly different from results with any other probe tested. Most importantly, the intensity of the hybridization to RNA from G2A infections is reduced by 5- to 10-fold compared with a wt infection. Thus, sequences representing the 3′ end of a large gene are present in reduced amounts in the G2A infection. Interestingly, the RNAs detected by the A10L 3′ probe in a G2A infection are not reduced in size relative to the wt infection. This observation is consistent with the interpretation that the A10L 3′ probe detects a small quantity of RNA that is initiated properly at the A10L promoter and extended to the end of the A10L coding region. Interestingly, the absolute sizes of the F17R and A10L mRNAs are different in wt-infected cells but similar in G2A-infected cells. Specifically, in wt-infected cells, the bulk of the F17R mRNA is approximately 2 kb in length and the A10L mRNA is approximately 3 kb in length, whereas in G2A infected cells, the RNAs from both genes are 300 to 1,500 nt in length. In summary, these results support the hypothesis that the reduction in mRNA size observed in G2R mutant infections represents a truncation of mRNA 3′ ends.

To further confirm and more precisely quantify the truncation of RNA 3′ ends, RNase protection analysis was done with the same gene, F17R and A10L, 5′ and 3′ probes used in the assays described above (Table 1, probes 4 to 7). Because these probes do not contain 5′ and 3′ untranslated sequence, the protected fragments produced in these experiments represent complete protection of the viral sequence contained in each probe. The intensities of the signal detected with the F17R 5′

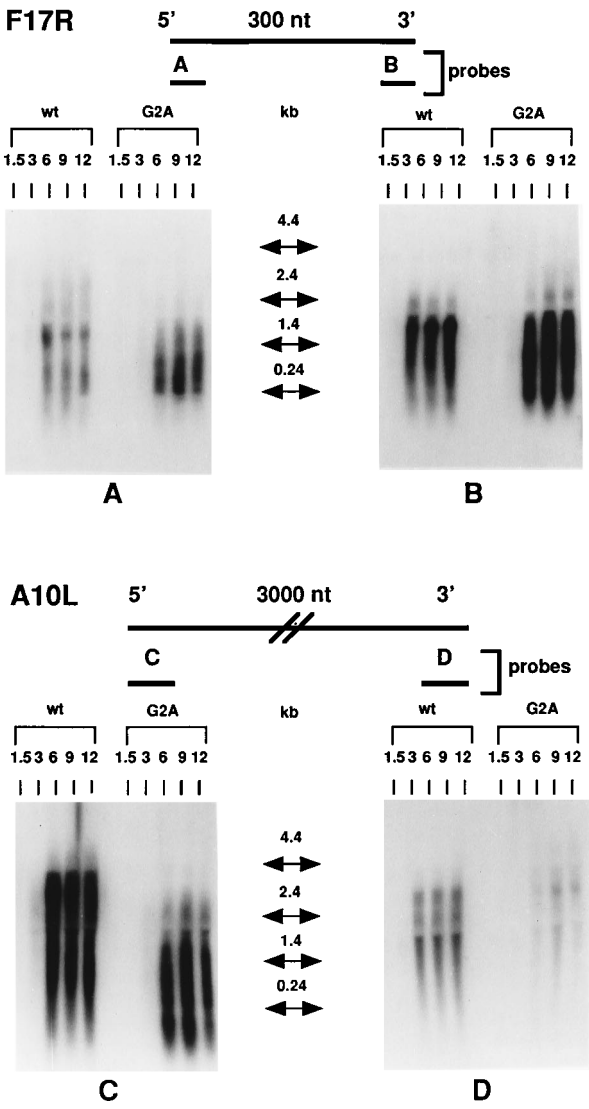

FIG. 5. Northern blot analysis of the A10L and F17R transcripts. Total RNA was isolated from wt- or G2A mutant-infected cells at the times indicated, fractionated on formaldehyde-agarose gels, and transferred to GeneScreen membranes. The blots were probed with a uniformly labeled antisense RNA riboprobe specific for the 5′ end of the F17R open reading frame (Table 1, probe 6) (A), the 3′ end of the F17R open reading frame (Table 1, probe 7) (B), the 5′ end of the A10L open reading frame (Table 1, probe 4) (C), or the 3′ end of the A10L open reading frame (Table 1, probe 5) (D). The diagrams above the lanes illustrate the sizes of the genes (not to scale) and specificities of the corresponding riboprobes.

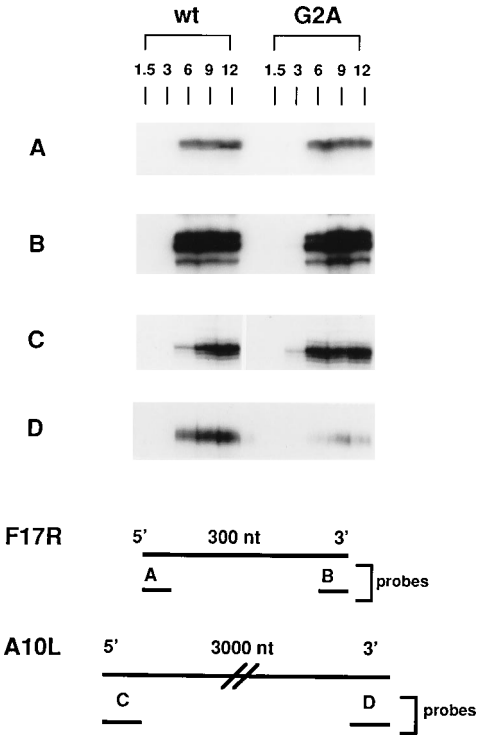

FIG. 6. RNase protection analysis of the 5′ and 3′ ends of the A10L and F17R open reading frames. Total RNA was isolated from wt- or G2A-infected cells and hybridized to uniformly labeled antisense riboprobes specific for the 5′ end of F17R (Table 1, probe 6) (A), the 3′ end of F17R (Table 1, probe 7) (B), the 5′ end of A10L (Table 1, probe 4) (C), or the 3′ end of A10L (Table 1, probe 5) (D). Following RNase digestion, the protected probe fragments were analyzed by denaturing PAGE and autoradiography. The diagrams at the bottom show the sizes of the genes and positions of the probes.

and 3′ probes and with the A10L 5′ probe were identical in the wt and G2A infections (Fig. 6A to C). Consistent with the results of the Northern blot analysis (Fig. 5D), the intensity of the signal detected with the A10L 3′ probe was 5- to 10-fold less in the G2A infection than in the wt infection (Fig. 6D).

One possible explanation for the observed truncation of RNA 3′ ends described above is that the processivity of the RNA polymerase during intermediate and late transcription is compromised in G2R mutant infections. Were this the case, then one would expect that compared with a wt infection, in a G2R mutant infection, the quantity of RNA from any intermediate or late transcription unit would decrease as a function of distance from the transcription start site. We therefore assayed transcription across the entire A10L coding sequence by RNase protection, using a series of uniformly labeled, nonoverlapping antisense riboprobes (Fig. 7 and Table 1, probes 8 to 11). Riboprobes were constructed such that the 5′-proximal probe produced a relatively small protected fragment, and the size of the protected fragment increased as a function of distance from the 5′ end. As in the RNase protection experiment described above (Fig. 6), the protected fragments represent complete protection of the viral sequences contained in the riboprobe; the reduction in size of each probe observed during RNase digestion represents removal of nonviral sequences from the probe. RNA was purified at 12 h postinfection from cells infected with wt virus at 31, 37, and 40°C, with C*ts*56 at 31 and 40°C, or with G2A at 37°C. Total RNA was hybridized to a mixture containing an excess of each of the four riboprobes, and RNase-resistant fragments were analyzed by PAGE and autoradiography (Fig. 7A). The protected fragments for each probe were quantified with a PhosphorImager, and the results are expressed as a ratio of arbitrary units of radioactivity under each nonpermissive condition to the arbitrary units of radioactivity under the relevant permissive condition. The results confirm that compared with wt infections, in G2R mutant infections, the steady-state quantity of A10L RNA present in infected cells decreases as a function of distance from the transcription start site.

DISCUSSION

Our in vivo characterization of vaccinia virus G2R mutants demonstrates that the G2R gene plays an essential role in viral

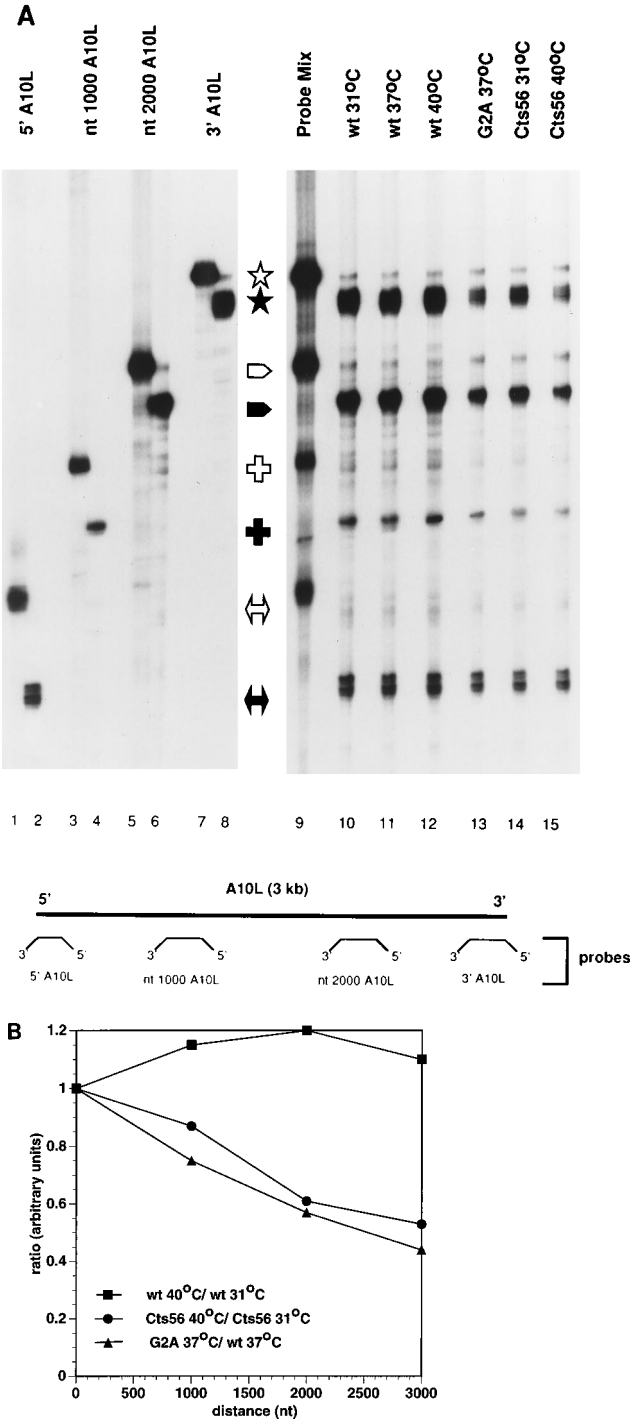

FIG. 7. RNase protection analysis of transcription across the A10L open reading frame. (A) For lanes 1 to 8, total RNA was isolated from wt-infected cells at 12 h postinfection. RNA was hybridized to the 5′ A10L probe (lane 2), the nt 1000 A10L probe (lane 4), the nt 2000 A10L probe (lane 6), or the 3′ A10L probe (lane 8) and digested with RNase in high salt, and the protected fragments were electrophoresed on a denaturing polyacrylamide gel. Undigested riboprobes were electrophoresed in lane 1 (5′ A10L), lane 3 (nt 1000 A10L), lane 5 (nt 2000 A10L), and lane 7 (3′ A10L). A mixture of the four undigested riboprobes was electrophoresed in lane 9. For lanes 10 to 15, total RNA was isolated at 12 h postinfection from wt virus-infected cells at 31°C (lane 10), wt virus-infected cells at 37°C (lane 11), wt virus-infected cells at 40°C (lane 12), G2A virus-infected cells at 37°C (lane 13), C*ts*56 virus-infected cells at 31°C (lane 14), or C*ts*56 virus-infected cells at 40°C (lane 15). RNA was hybridized to the probe mix and digested with RNase in high salt, and the protected fragments were electrophoresed on a denaturing polyacrylamide gel. Undigested riboprobes are indicated by open symbols, and the protected fragments are indicated with the corresponding filled symbols. The diagram at the bottom shows the position of each probe (not to scale) relative to the coding sequence for the A10L gene. (B) Protected fragments in lanes 10 to 15 of panel A were quantitated by PhosphorImager analysis. Data were normalized for the number of radiolabeled cytosine residues incorporated in each protected fragment. For each lane, the 5′-end protected fragment was arbitrarily assigned a value of 1, and values for the remaining fragments were then normalized to that value. The ratios of the values obtained for protected fragments under nonpermissive and permissive conditions were next determined and are presented graphically.

mRNA metabolism. During G2R mutant infections, initiation of early, intermediate, and late gene transcription appears to be normal and early mRNA structure is unaffected, while intermediate and late mRNAs are reduced in size. The observed reduction in mRNA size represents a truncation of mRNA 3′ ends. The limited reduction in the size of intermediate and late viral mRNAs accounts for the fact that late during G2R mutant infections, small proteins are synthesized in normal amounts while large proteins are synthesized in reduced quantities. There are three possible explanations for the effects of G2R mutants on mRNA size. First, it is possible that the G2R protein normally functions in DNA metabolism and that in the absence of G2R function, the viral DNA template is damaged in a fashion that results in premature termination of intermediate and late gene transcription. Second, it is possible that the abnormally short mRNAs result from increased degradation of mRNA 3′ ends. Finally, it is possible that the truncation of mRNA 3′ ends observed in G2R mutant infections results from a decrease in the elongation potential of the viral RNA polymerase. Our experiments do not eliminate the first two possibilities. However, we favor the hypothesis that the G2R gene affects synthesis of mRNA 3′ ends since other genetic experiments, described below, suggest that the G2R protein directly affects transcription. Ultimately, proof of this hypothesis will require a rigorous biochemical definition of the activity of the G2R protein.

To date, very little is known about the mechanism of formation of intermediate and late vaccinia virus mRNA 3′ ends. The structures of intermediate and late mRNAs imply that once initiated, the vaccinia virus RNA polymerase terminates at a very large number of sites between 1 and 4 kb downstream of the promoter. Our results imply that this process is influenced by the activity of the G2R gene. Specifically, the phenotype of the G2R mutants implies that during a wt infection, the G2R gene product enhances transcription elongation. Numerous examples of control of transcription elongation have been reported (12). The efficiency of elongation by eucaryotic RNA polymerase II is increased by the factors TFIIS (humans), SII (mice), and DmSII (*Drosophila* spp.), which act by suppressing RNA polymerase pausing at *cis*-acting elements. During human immunodeficiency virus infection, the efficiency of elongation by RNA polymerase II is increased by the Tat protein, which acts by modulation of the initiation complex assembled at the viral long terminal repeat. During bacteriophage lambda infection, RNA polymerase elongation is regulated by competition between an N-protein-mediated antitermination complex and an inhibitor of antitermination. Interestingly, one subunit of the vaccinia virus RNA polymerase, E4L, which is also required for specific initiation of intermediate gene transcription, exhibits limited homology to the human transcription elongation factor TFIIS (23). It is interesting to speculate that E4L, G2R, and perhaps other vaccinia virus gene products act together to regulate transcription elongation by using mechanism(s) analogous to those described above.

Consideration of the IBT dependence phenotype of lethal G2R mutations implicates specific vaccinia virus genes in an interaction with the G2R gene product. In wt-infected cells, IBT induces promiscuous transcription, that is, transcriptional activation late during infection of regions of the genome which are normally transcriptionally silent (3). Interestingly, *ts* mutations in the vaccinia virus gene A18R, which encodes a DNA helicase (27), result in a promiscuous transcription phenotype which is indistinguishable from the effects of IBT on a wt infection (3). Since lethal mutation of G2R compensates for promiscuous transcription induced by IBT, and since lethal mutation of A18R also induces promiscuous transcription, it seems likely that mutation of G2R can compensate for defects in A18R. In fact, we have recently succeeded in constructing viable recombinants of vaccinia virus which contain both a *ts* mutation in A18R and a deletion mutation in G2R, and we have shown that second-site phenotypic revertants of A18R *ts* mutants which map to G2R can be isolated (8). These results suggest that the A18R and G2R proteins interact and that their activities are complementary in vivo. Finally, it is noteworthy that mutation of the second-largest subunit of the viral RNA polymerase can induce resistance to IBT (4), reinforcing the hypothesis that IBT, G2R, and A18R all directly affect transcription. In summary, we speculate that the G2R protein may interact directly with the A18R protein and that the complex of these two proteins may interact with the viral RNA polymerase to modulate transcription elongation.

Precise biochemical characterization of the activity of the G2R gene product will require reproduction of the in vivo phenotype described here in an in vitro biochemical assay. To date, the in vitro assays which have been used to study vaccinia virus transcription have been constructed such that they are sensitive to factors affecting primarily transcription initiation but not elongation. Thus, fractionation of extracts from vaccinia virus virions or infected cells has resulted in the identification of many of the factors necessary for initiation of each specific class of vaccinia virus genes (20). The G2R and A18R proteins are conspicuously absent from the inventory of vaccinia virus transcription factors purified to date. Biochemical experiments designed to measure the activity of the G2R protein in vitro are under way.

ACKNOWLEDGMENTS

We thank Bernard Moss and Anna Ramsey-Ewing for reagents and protocols provided during the course of this work and David Simpson for critical reading of the manuscript. The PhosphorImager analysis equipment and oligonucleotides were provided by the University of Florida DNA core facility.

This work was supported by National Institutes of Health grant AI18094 (R.C.C.).

REFERENCES

1. **Baldick, C. J., Jr., J. G. Keck, and B. Moss.** 1992. Mutational analysis of the core, spacer, and initiator regions of vaccinia virus intermediate-class promoters. J. Virol. **66:**4710–4719.
2. **Baldick, C. J., Jr. and B. Moss.** 1993. Characterization and temporal regulation of mRNAs encoded by vaccinia virus intermediate-stage genes. J. Virol. **67:**3515–3527.
3. **Bayliss, C. D., and R. C. Condit.** 1993. Temperature-sensitive mutants in the vaccinia virus A18R gene increase double-stranded RNA synthesis as a result of aberrant viral transcription. Virology **194:**254–262.
4. **Condit, R. C., R. Easterly, R. F. Pacha, Z. Fathi, and R. J. Meis.** 1991. A vaccinia virus isatin-β-thiosemicarbazone resistance mutation maps in the viral gene encoding the 132-kDa subunit of RNA polymerase. Virology **185:**857–861.
5. **Condit, R. C., and A. Motyczka.** 1981. Isolation and preliminary characterization of temperature-sensitive mutants of vaccinia virus. Virology **113:**224–241.
6. **Condit, R. C., A. Motyczka, and G. Spizz.** 1983. Isolation, characterization, and physical mapping of temperature-sensitive mutants of vaccinia virus. Virology **128:**429–443.
7. **Condit, R. C., and E. G. Niles.** 1990. Orthopoxvirus genetics. Curr. Top. Microbiol. Immunol. **163:**1–40.
8. **Condit, R. C., Y. Xiang, and J. I. Lewis.** 1995. Unpublished data.
9. **Ensinger, M. J.** 1987. Phenotypic characterization of temperature-sensitive mutants of vaccinia virus with mutations in a 135,000-M_r subunit of the virion-associated DNA-dependent RNA polymerase. J. Virol. **61:**1842–1850.
10. **Feinberg, A. P., and B. Vogelstein.** 1984. A technique for radiolabeling DNA restriction endonuclease fragments to high specific activity. Addendum. Anal. Biochem. **137:**266–267.
11. **Hassett, D. E., and R. C. Condit.** 1994. Targeted construction of temperature-sensitive mutations in vaccinia virus by replacing clustered charged residues with alanine. Proc. Natl. Acad. Sci. USA **91:**4554–4558.
12. **Kane, C. M.** 1994. Transcript elongation and gene regulation in eukaryotes, p. 279–296. *In* R. C. Conaway and J. W. Conaway (ed.), Transcription: mechanisms and regulation. Raven Press, New York.
13. **Kovacs, G. R., R. Rosales, J. G. Keck, and B. Moss.** 1994. Modification of the cascade model for regulation of vaccinia virus gene expression: purification of a prereplicative, late-stage-specific transcription factor. J. Virol. **68:**3443–3447.
14. **Laemmli, U. K.** 1970. Cleavage of structural proteins during assembly of the head of bacteriophage T4. Nature (London) **227:**680–685.
15. **Mahr, A., and B. E. Roberts.** 1984. Arrangement of late RNAs transcribed from a 7.1-kilobase *Eco*RI vaccinia virus DNA fragment. J. Virol. **49:**510–520.
16. **Meis, R. J.** 1990. Molecular biological and phenotypic characterization of a vaccinia virus gene which renders the virus dependent on isatin-beta-thiosemicarbazone (IBT). PhD thesis. State University of New York, Buffalo.
17. **Meis, R. J., and R. C. Condit.** 1991. Genetic and molecular biological characterization of a vaccinia virus gene which renders the virus dependent on isatin-β-thiosemicarbazone (IBT). Virology **182:**442–454.
18. **Milligan, J. F., D. R. Groebe, G. W. Witherell, and O. C. Uhlenbeck.** 1987. Oligoribonucleotide synthesis using T7 RNA polymerase and synthetic DNA templates. Nucleic Acids Res. **15:**8783–8798.
19. **Moss, B.** 1990. Poxviridae and their replication, p. 2079–2112. *In* B. N. Fields, D. M. Knipe, R. M. Chanock, M. S. Hirsch, J. L. Melnick, T. P. Monath, and B. Roizman (ed.), Virology. Raven Press, New York.
20. **Moss, B., B. Y. Ahn, B. Amegadzie, P. D. Gershon, and J. G. Keck.** 1991. Cytoplasmic transcription system encoded by vaccinia virus. J. Biol. Chem. **266:**1355–1358.
21. **Moyer, R. W.** 1987. The role of the host cell nucleus in vaccinia virus morphogenesis. Virus Res. **8:**173–191.
22. **Pacha, R. F., and R. C. Condit.** 1985. Characterization of a temperature-sensitive mutant of vaccinia virus reveals a novel function that prevents virus-induced breakdown of RNA. J. Virol. **56:**395–403.
23. **Rosales, R., N. Harris, B. Y. Ahn, and B. Moss.** 1994. Purification and identification of a vaccinia virus-encoded intermediate stage promoter-specific transcription factor that has homology to eukaryotic transcription factor SII (TFIIS) and an additional role as a viral RNA polymerase subunit. J. Biol. Chem. **269:**14260–14267.
24. **Rosales, R., G. Sutter, and B. Moss.** 1994. A cellular factor is required for transcription of vaccinia viral intermediate-stage genes. Proc. Natl. Acad. Sci. USA **91:**3794–3798.
25. **Sambrook, J., E. F. Fritsch, and T. Maniatis.** 1989. Molecular cloning: a laboratory manual, 2nd ed. Cold Spring Harbor Laboratory Press, Cold Spring Harbor, N.Y.
26. **Shuman, S., S. S. Broyles, and B. Moss.** 1987. Purification and characterization of a transcription termination factor from vaccinia virions. J. Biol. Chem. **262:**12372–12380.
27. **Simpson, D. A., and R. C. Condit.** 1995. Vaccinia virus gene A18R encodes an essential DNA helicase. J. Virol. **69:**6131–6139.
28. **Yuen, L., and B. Moss.** 1987. Oligonucleotide sequence signaling transcriptional termination of vaccinia virus early genes. Proc. Natl. Acad. Sci. USA **84:**6417–6421.